SECOND EUROPEAN CONFERENCE ON EARTHQUAKE ENGINEERING AND SEISMOLOGY, ISTANBUL AUG. 25-29, 2014

Turkish Earthquake Foundation - Earthquake Engineering Committee
Prime Ministry, Disaster And Emergency Management Presidency

OBSERVATIONS FROM A LARGE SCALE SHAKE TABLE TEST ON A MODEL OF EXISTING PILE-SUPPORTED MARINE STRUCTURE SUBJECTED TO LIQUEFACTION INDUCED LATERAL SPREADING

S. Mohsen HAERI[1], Ali KAVAND[2], Javad RAISIANZADEH[3], Hadi PADASH[4], Iraj RAHMANI[5], Ali BAKHSHI[6]

ABSTRACT

This paper aims to study the effects of liquefaction induced lateral spreading on the piles of a marine dolphin located in a port at south of Iran. For this purpose, a large scale 1g shake table test is conducted on the physical model of the marine dolphin. The physical model was shaken with scaled Bam earthquake record that induced liquefaction and lateral spreading in the model. Different parameters including time-histories of accelerations, pore water pressures and displacements in free field as well as the displacement at the pile cap and the bending moments in the piles were recorded and analyzed. The analysis indicated large induced bending moments in the piles. Besides, lateral pressures on the model piles were back-calculated from the bending moment data. The results reveal that the magnitude and pattern of lateral pressure on the piles as well as the bending moments vary depending on the pile position within the group. Experimental active lateral pressures due to lateral spreading on downslope piles of the group can reasonably be predicted by the formulations of the design codes provided that the depth of significant movement of liquefied soil during lateral spreading is correctly evaluated and used in calculations. In this regard, prediction of the passive pressures at lower depths of piles obtained by the experimental results is beyond the scope of the design code and should separately be evaluated and considered in practice. It is concluded that although the piles of marine dolphin were able to withstand the exerted bending moments due to the lateral spreading, the amount of residual displacement at the pile cap was not within the acceptable range to satisfy the performance criteria.

INTRODUCTION

Coastal areas in seismically active regions are prone to development of liquefaction and subsequent lateral spreading due to the earthquakes induced excess pore water pressure in saturated loose sandy soils that are usually present near shores. Lateral spreading usually occurs in mildly sloping grounds or those ending in free faces (e.g. coastal waterfronts or river banks) as a consequence of liquefaction. Lateral spreading is recognized as a destructive phenomenon since the lateral displacements during lateral spreading can reach to several meters, imposing large lateral pressures on pile foundations of the structures.

[1] Professor, Civil Engineering Department, Sharif University of Technology, Tehran, Iran, smhaeri@sharif.edu
[2] Assistant Professor, School of Civil Engineering, College of Engineering, University of Tehran, Tehran, Iran
[3] PhD Student, School of Civil Engineering, College of Engineering, University of Tehran, Tehran, Iran
[4] MSc Graduate, Civil Engineering Department, Sharif University of Technology, Tehran, Iran
[5] Assistant Professor, Transportation Research Institute, Iran University of Science and Technology, Tehran, Iran
[6] Assistant Professor, Civil Engineering Department, Sharif University of Technology, Tehran, Iran

During past earthquakes, several examples of severe damages to pile supported structures due to lateral spreading have been reported. In this respect, the cases in the 1964 Niigata (Hamada et al., 1986), the 1995 Kobe (Tokimatsu and Asaka, 1998) and the 2010 Haiti earthquakes (Eberhard et al., 2010) are among the most destructive ones. These evidences have motivated researchers in the field of earthquake geotechnical engineering to investigate the lateral spreading phenomenon and specially its effects on the deep foundations of structures through experimental or numerical studies. On this subject, experimental investigations have been conducted by shaking table, centrifuge and field tests (e.g. Haeri et al. 2012, Motamed and Towhata 2010, Gonzalez et al. 2009, Abdoun et al. 2003, Ashford et al. 2006) during previous studies. Because of the complicated mechanism of soil-pile interaction in laterally spreading ground, different aspects of this problem have not yet been understood and thus it demands for further investigations. For instance, experimental investigations on the behavior of pile groups behind quay walls which were conducted by Motamed and Towhata (2010) have shown that the values of the lateral pressures from the liquefied layer against individual piles of a group vary depending on the position of piles within the group. Recently, Haeri et al. (2012) based on the results of a large scale 1g shake table test, showed that both magnitude and pattern of lateral pressures due to lateral spreading on individual piles of a group of piles without pile cap in an infinite mild slope far from a free face vary based on the position of pile in the group because of the shadow and neighboring effects but the trend of this variation is different from those previously reported by other investigators for pile groups located behind a quay wall or close to a free face. However, these observations are limited to the regular configurations of pile groups (i.e. n□n or n□m piles in square or rectangular configurations) and there is no detailed information regarding the cases with specific configurations such as a triangular pile configuration commonly implemented for marine structures.

In this paper the effects of liquefaction induced lateral spreading on an existing pile-supported marine dolphin located in a port at south of Iran is investigated. For this purpose, a large scale 1g shake table test is conducted on the physical model of the marine dolphin. The piles of the marine dolphin were arranged in a triangular configuration like that of the prototype. Various parameters of the response of laterally spreading soil such as acceleration, pore water pressure and displacements as well as those of the pile group including bending moments and deflections were recorded during the experiment that are presented and discussed in this paper. A detailed analysis is also conducted to determine and compare lateral pressure of liquefied soil on piles during lateral spreading.

PHYSICAL MODEL

The experiment of this study was conducted by the shaking table device of the Earthquake Engineering Research Center at Sharif University of Technology (SUT).

The physical model was constructed and tested in a rigid box which had a length of 3.5 m, width of 1 m and height of 1.5 m. Fig.1 shows the schematic cross section and plan view of the physical model along with the layout of transducers. According to this Figure, the soil profile consists of a 1.2m thick liquefiable layer consisting of loose sand with relative density of about 15% overlying a bottom non-liquefiable dense sand layer having 25 cm thickness and relative density of about 80%. All the soil layers have a slope of 7%. The sand used in physical model is standard Firoozkuh silica sand (No. 161) with a golden yellow appearance and a uniform gradation that is widely used in Iran for geotechnical testing.

The piles of prototype marine dolphin are steel pipes having an outer diameter of 2.0m and thickness of 3.8cm. The scale similitude laws proposed by Iai (1989) and Iai et al. (2005) were used to calculate mechanical and geometrical properties of the piles in model scale. For this purpose, the geometrical scale was selected as □=10 (prototype/model). All model piles were made of aluminum pipes. Material properties of the model piles are summarized in Table 1.

As sketched in Figure 1, different types of transducers were employed in the physical model including accelerometers and pore pressure transducers in the free field (far from the piles) to measure soil accelerations and excess pore water pressures, respectively; pore pressure transducers close to the piles to monitor build-up and dissipation of the excess pore pressures in the near field (close to the piles); displacement transducers (LVDTs) attached to the pile cap and also in free field to record pile

and soil lateral displacements and finally strain gauges pasted along the piles to record bending moments in piles. The base shaking was scaled Bam earthquake record with PGA of 0.25g and a reduced duration of 17 sec that was applied to the model parallel to the ground slope.

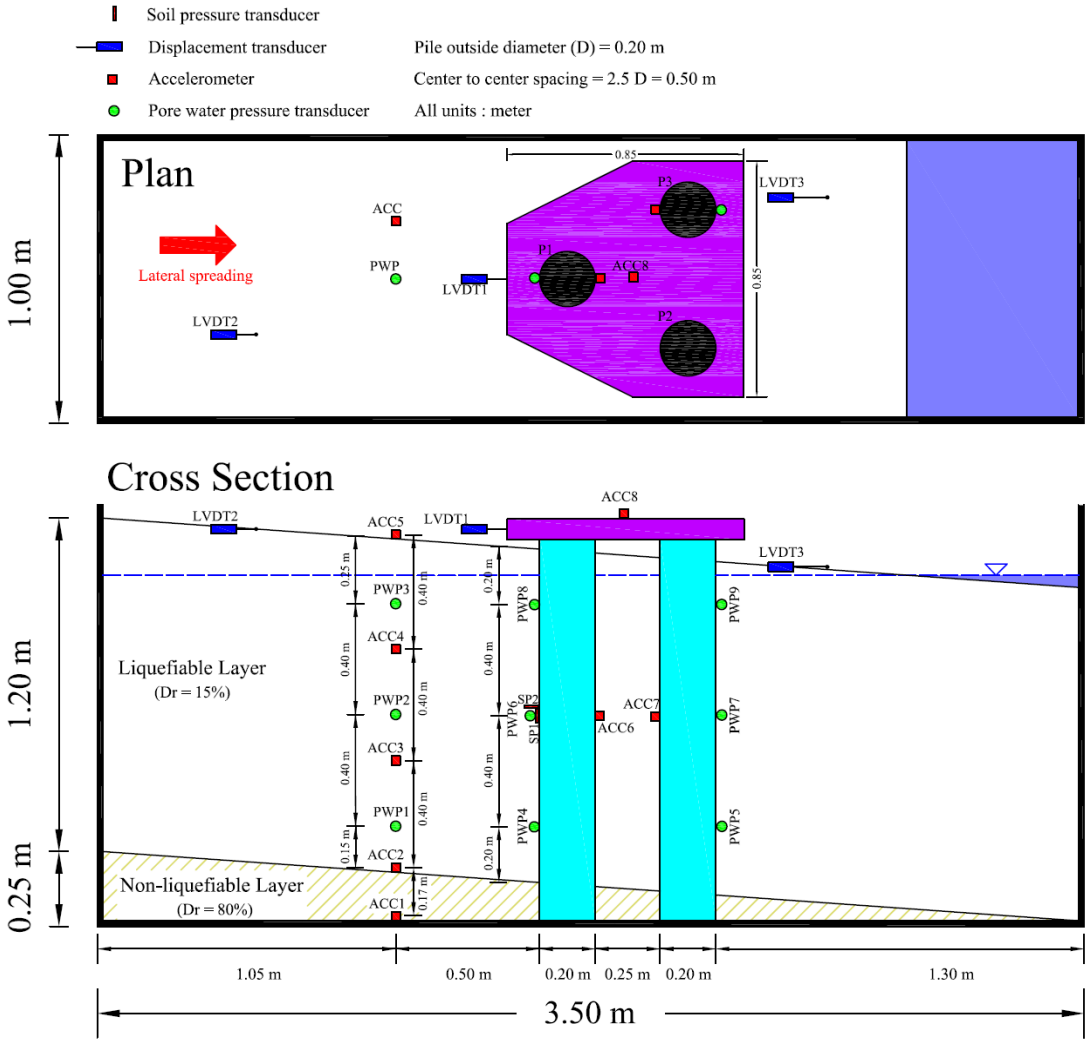

Figure 1. Plan view and cross section of physical model along with the layout of transducers

Table 1. Mechanical and geometrical properties of model piles

Material	Height (m)	Outer/inner diameter (cm)	I (cm^4)	EI ($kN.m^2$)
Aluminum	1.40	20.0/19.8	309.48	217.58

GENERAL EXPERIMENTAL RESULTS

A summary of the main data measured during the test is presented and discussed in this section. Representative acceleration time histories of the soil in the free field part of the model (soil far from the piles) are shown in Figure 2. According to this figure, upon soil liquefaction at the beginning stages of shaking, the amplitude of acceleration records in liquefiable layer decreases and the frequency contents of the records alter dramatically.

Sample time histories of excess pore water pressure records in free field soil are presented in Figure 3. As seen, the soil liquefies at the beginning of the shaking and the upper the elevation of the point in concern, the sooner the initiation of the liquefaction. In this regard, it should be noted that at the depth of 1.05 m (location of PWP1) the excess pore water pressure reaches the initial overburden stress nearly at the end of shaking and after that the drainage of excess pore pressure immediately

starts. In other words, high values of excess pore water pressure in lower depths are observed for a much shorter duration than those observed for upper depths. Drainage of excess pore water pressure initiated from the lower depths (PWP1) followed by reduction of pore pressure in upper elevations (PWP2 and PWP3).

Time histories of lateral displacements of ground surface and pile cap during lateral spreading are shown in Figure 4. As seen, the soil started to move toward downslope at the beginning of shaking after liquefaction. The maximum ground surface displacement is about 4.5cm observed at the end of shaking. The maximum lateral displacement of the pile cap is about 2.5cm that occurs at the middle of shaking and by continuation of shaking, the piles gradually bounce back. However, the amount of this bouncing back is small so that the residual displacement of the pile cap at the end of shaking is about 2.0cm which is not within the acceptable range to satisfy the performance criteria of the structure.

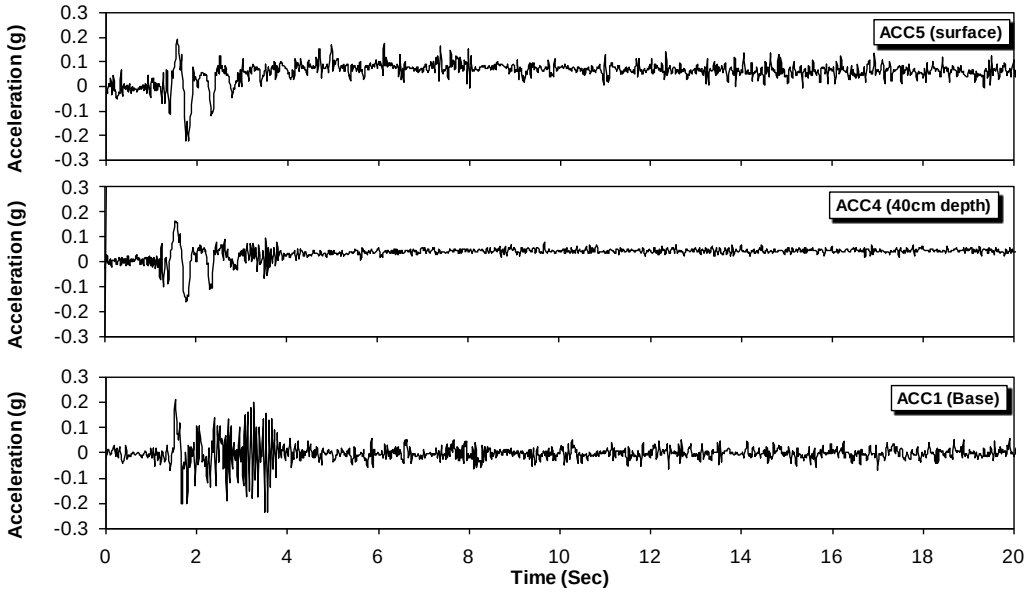

Figure 2. Acceleration time histories of soil in free field

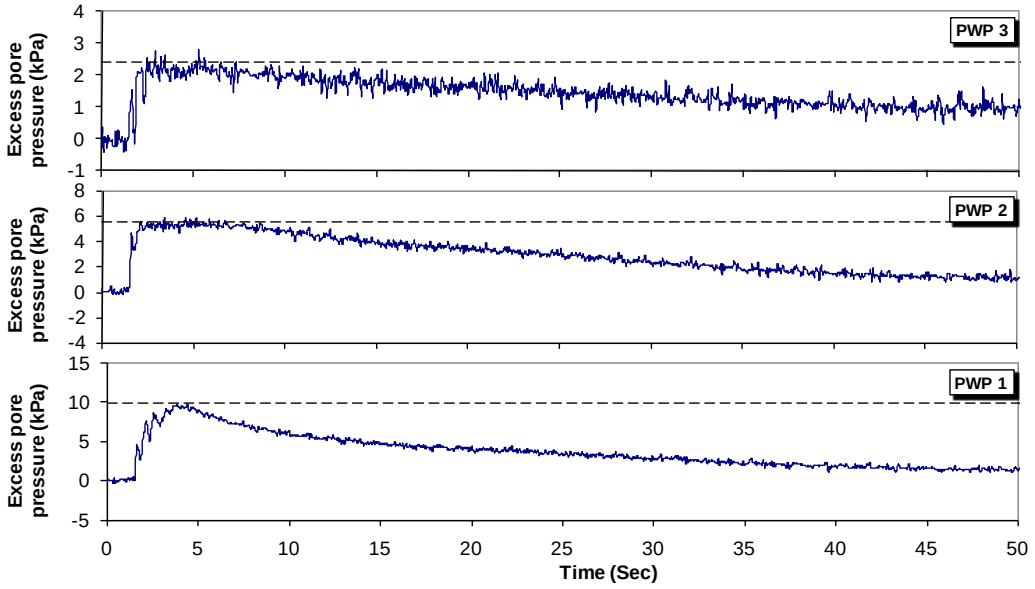

Figure 3. Sample excess pore water pressure records in free field

Time histories of bending moments in the individual piles of the group at two representative depths (at the base of liquefiable layer and close to the pile cap) are presented in Figure 5. Pile 1 is located at the upslope side of the group while piles 2 and 3 are located at the downslope. According to Figure 5, after lateral spreading bending moment in piles increases and reaches its peak value at about

t=2.34sec. However, during liquefaction, the soil loses most of its shear strength; therefore it fails and gradually moves around the piles. This movement reduces the lateral pressure on the piles allowing them to return towards upslope due to their stiffness as the shaking continued. Due to this elastic rebound, bending moment in piles decreases as well. It should be noted that time histories of bending moments in piles consist of a dynamic component due to dynamic soil pressures and a monotonic component from the kinematic lateral soil pressures during lateral spreading.

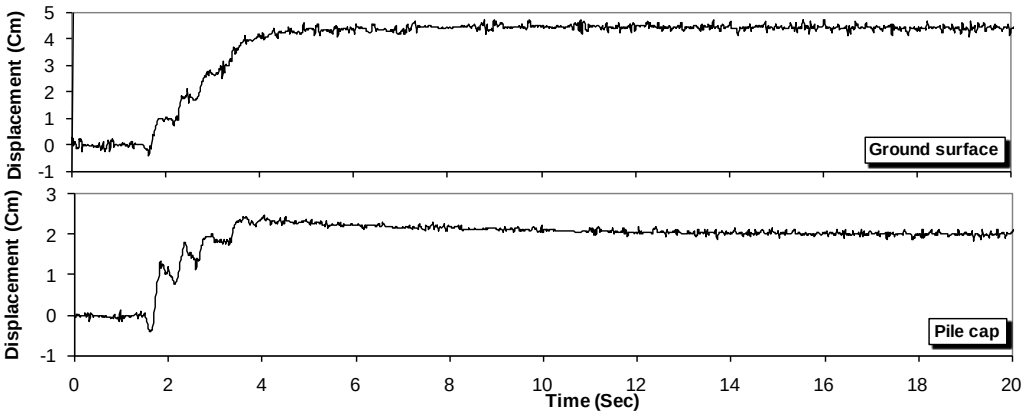

Figure 4. Time histories of lateral displacements of ground surface and pile cap

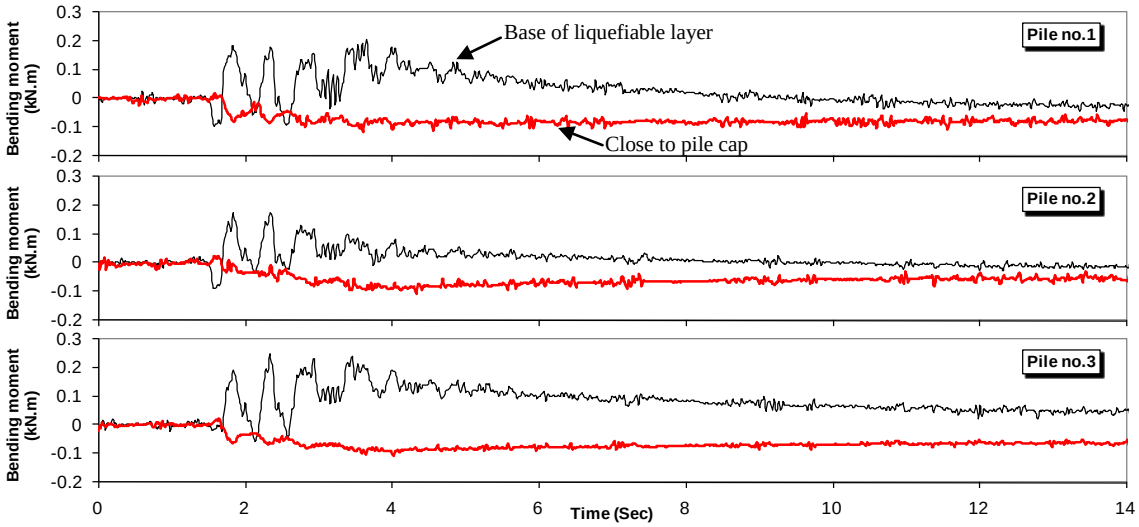

Figure 5. Sample time histories of bending moments in individual piles of the group

Figure 6 displays profile of bending moments in piles at selected time steps during lateral spreading. As seen, bending moments at the base and top (near the cap) of the piles have opposite directions. This is due to the constraint applied by the cap to the top of the piles. In all piles the maximum positive bending moment occurs at a depth near the base of liquefiable layer while the maximum negative bending moment is observed near the connection of piles to the cap. Comparing maximum positive bending moments in piles reveals that downslope piles (P2 and P3) experienced larger bending moments than upslope pile (P1). The maximum positive bending moments in piles P2 and P3 are respectively about 1.40 and 1.55 times that observed for pile P1. Also the trend of variation of bending moment for pile P1 was different from piles P2 and P3. In other words, the trend and the maximum bending moments varied in individual piles of the group depending on their position within the group.

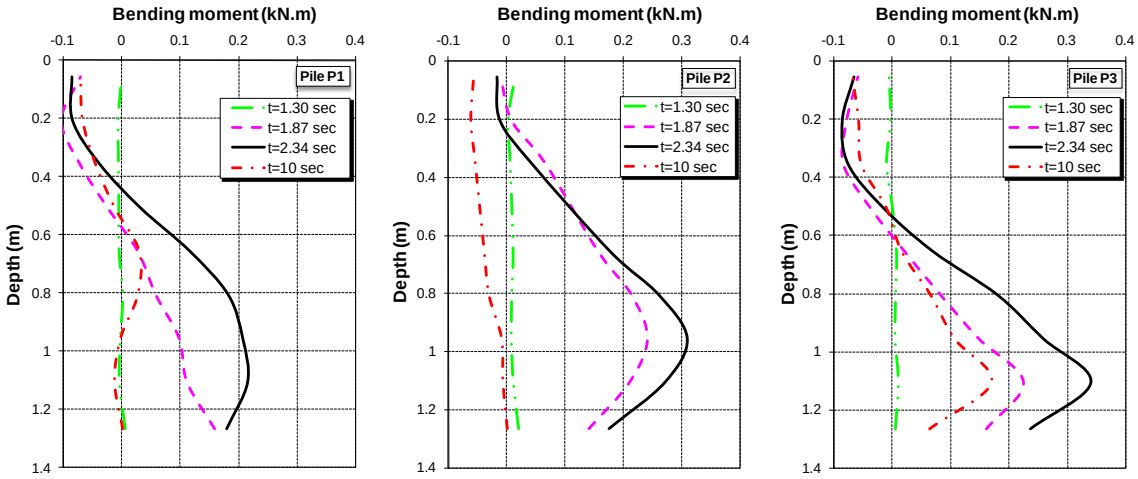

Figure 6. Variation of bending moments with depth in individual piles of the group at selected snapshots during lateral spreading

LATERAL PRESSURE OF SOIL ON PILES DUE TO LATERAL SPREADING

Determination of lateral pressure of liquefied soil on the piles during lateral spreading is a subject of interest to geotechnical designers. The lateral pressures exerted on the piles of the group were back-calculated from the bending moment data using a double differentiation procedure ($P(z)=d^2M/dz^2$) optimized for minimization of numerical errors as introduced by Brandenberg et al. (2010).

Figure 7 shows time histories of back-calculated soil pressures on piles during lateral spreading at two representative depths. It should be noted that these time histories contain both monotonic component induced by lateral spreading of liquefied soil as well as dynamic component due to the ground oscillations during shaking. According to Figure 7, lateral pressure on the piles increases as lateral spreading occurs and attains a peak value between t=2.0 sec and t=4.0 sec while most of the lateral movement of liquefied soil occurs. After lateral spreading, the values of soil lateral pressures decrease and approach to zero except at lower depths of rear piles (no.2 & no.3) where some amount of residual pressures are observed.

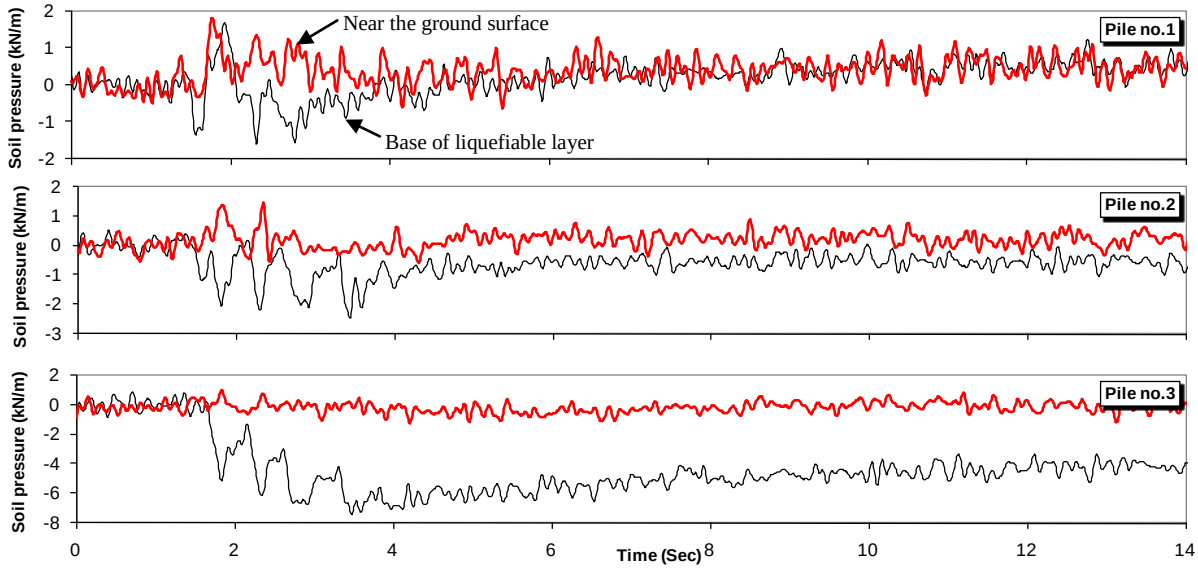

Figure 7. Sample time histories of soil lateral pressure on individual piles of the group during lateral spreading

Figure 8 displays profiles of lateral pressure of liquefied soil on piles drawn at the same time steps previously presented in Figure 6 for bending moments. In this figure, positive values show active pressures on piles that are due to lateral movement of liquefied soil during lateral spreading while negative pressures represent passive pressure that resists against pile movement. As seen, the lateral pressures at the base and top of the piles have opposite directions. In other words, at the upper half of the liquefied layer, active pressure is observed while at the lower half, passive pressure develops. This observation can be interpreted by the fact that the amount of soil displacement at the lower half of liquefiable layer is less than that at the upper half. As a result, as the pile undergoes lateral deflection, the soil at the lower half resist against the pile movement developing a passive pressure zone in lower depths. This finding is consistent with the trends previously observed in Figure 3 regarding the development of excess pore water pressure, which indicated that high values of excess pore water pressure are observed in a much shorter duration in lower depth compared to those in upper elevations. This means that the soil in lower depths does not completely lose its shear resistance during lateral spreading; hence being able to partially resist against lateral deflection of the piles. It should be added that the piles are short and stiff so they have rotated in addition to the bending deflections and ultimately due the smaller lateral movement of liquefied soil in lower depth, the piles experienced more passive pressures in bottom parts.

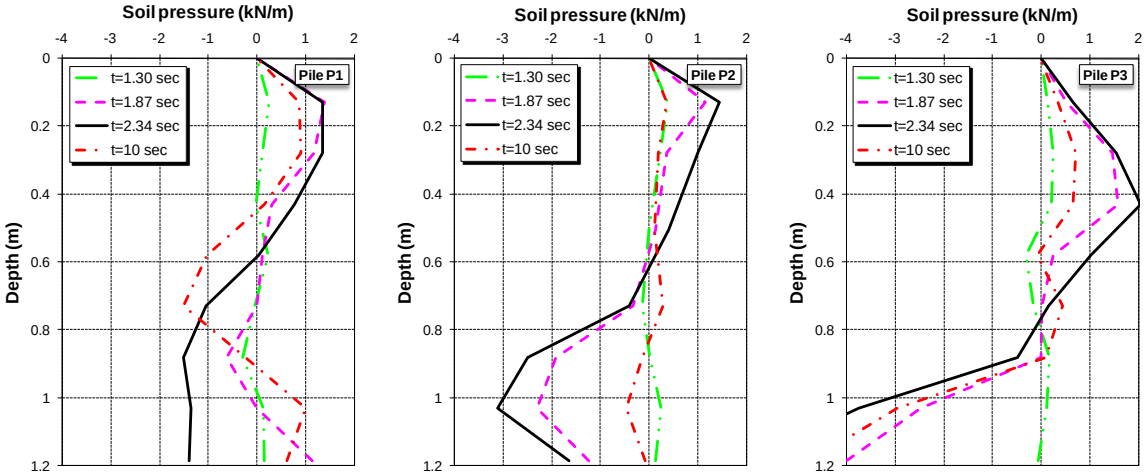

Figure 8. Profile of soil lateral pressure on piles at selected snapshots during lateral spreading

In Figure 9 a comparison is made between the maximum monotonic component of lateral pressure on individual piles of the group that happened about t=2.76 sec and the lateral pressure calculated based on the recommendations of JRA (2002) design code. This code proposes using 30% of the total overburden pressure to be applied to the outermost width of the pile group as lateral forces due to lateral spreading. For design applications, implementing JRA (2002), it is commonly assumed that the total lateral force exerted on the pile group is equally distributed among the piles in the group. As the piles in this study are configured in a triangular shape, the side of this triangle is selected as the width of the pile group that is equal to 0.65 m. Besides, the saturated density of the soil is equal to 19.6 kN/m^3, based on the data recorded during the construction of liquefiable layer in physical model. Referring to Figure 9, it is found that magnitude and pattern of the lateral pressures on piles 2 and 3 is consistent with the prediction by JRA (2002) up to a depth of about 0.6 m (i.e. the upper half of liquefied soil). In this respect, the disagreement in lower depths is interpreted by the fact that the prediction of JRA (2002) is based on the assumption that a considerable amount of lateral movement occurs in whole depths of liquefiable layer due to the lateral spreading while in current experiment, smaller lateral movement of liquefied soil in lower depths along with the rotation of piles lead to the development of more passive pressure against the bottom parts of the piles. For pile 1, the difference between lateral pressures recommended by JRA (2002) and the experimental result is significant both in terms of pattern and magnitude. Another obvious finding is that the pattern of lateral pressure distribution along the upslope pile (no.1) is different from those observed for the downslope piles (no.2&3).

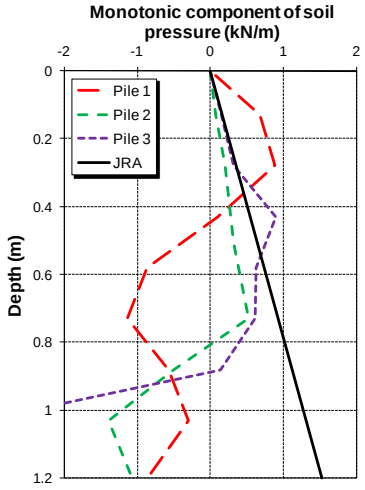

Figure 9. Comparison between monotonic component of maximum lateral pressure of liquefied soil on the piles and the corresponding values recommended by JRA design code

CONCLUSIONS

Findings from a large scale shake table test on physical model of a marine dolphin were presented and discussed. The results show that active lateral pressures due to lateral spreading on downslope piles of the group can be reasonably predicted by JRA (2002) design code provided that the depth of significant movement of liquefied soil during lateral spreading is correctly evaluated and used in calculations. However, for the upslope pile of the group, a major difference is observed between experimental lateral pressures and those calculated based on JRA (2002) both in terms of magnitude and pattern. It should be noted that calculations based on JRA (2002) fail to predict experimental passive pressures against the pile developed at the lower depths of liquefied layer since JRA (2002) formulations are based on a force-based method which only considers the active lateral pressures due to lateral spreading. This passive pressure against the piles at lower depths should be evaluated and considered in practice as well. There was a considerable difference between the pattern of lateral pressure distribution along the upslope pile of the group and that observed for downslope piles. It is also concluded that although the piles of the marine dolphin were able to withstand the induced bending moments due to the lateral spreading, the amount of residual displacement at the pile cap was not within the acceptable range to satisfy the performance criteria.

REFERENCES

Abdoun T, Dobry R, O'Rourke T, Goh SH (2003) "Pile response to lateral spreads: centrifuge modeling" *Journal of Geotechnical and Geoenvironmental Engineering*, 129(10): 869-678

Ashford SA, Juirnarongrit T, Sugano T, Hamada M (2006) "Soil–pile response to blast-induced lateral spreading. I: Field Test" *Journal of Geotechnical and Geoenvironmental Engineering*, 132(2):152-162

Brandenberg SJ, Wilson DW, Rashid MM (2010) "Weighted residual numerical differentiation algorithm applied to experimental bending moment data" *Journal of Geotechnical and Geoenvironmental Engineering*, 136(6):854-863

Eberhard Marc O, Baldridge S, Marshall J, Mooney W, Rix J (2010) The MW 7.0 Haiti Earthquake of January 12, 2010, TEAM REPORT V 1.1, USGS/EERI Advance Reconnaissance Team

Gonzalez L, Abdoun T, Dobry R (2009) "Effect of soil permeability on centrifuge modeling of pile response to lateral spreading" *Journal of Geotechnical and Geoenvironmental Engineering*, 35(1):62–73

Haeri SM, Kavand A, Rahmani I, Torabi H (2012) "Response of a group of piles to liquefaction-induced lateral spreading by large scale shake table testing" *Soil Dynamics and Earthquake Engineering*, 38:25-45

Hamada H, Yasuda S, Isoyama R, Emoto K (1986) Study on Liquefaction Induced Permanent Ground Displacements, Research report, Association for the Development of Earthquake Prediction, Japan

Iai S (1989) بSimilitude for shaking table tests on soilتstructureتfluid model in 1g gravitational fieldپ *Soils and Foundations*, 29(1):105ت118

Iai S, Tobita T, Nakahara T (2005) بGeneralized scaling relations for dynamic centrifuge testsپ *Geotechnique*, 55(5):355-362

JRA (2002) Seismic design specifications for highway bridges, Japan Road Association, English version, Prepared by Public Works Research Institute (PWRI) and Ministry of Land, Infrastructure and Transport, Tokyo, Japan

Motamed R and Towhata I (2010) بShaking table model tests on pile groups behind quay walls subjected to lateral spreadingپ *Journal of Geotechnical and Geoenvironmental Engineering*, 136(3):477-489

Tokimatsu K and Asaka Y (1998) بEffects of Liquefaction-Induced Ground Displacements on Pile Performance in the 1995 Hyogoken-Nambu Earthquakeپ *Special Issue of Soils and Foundations*, 163ت177